Two-Dimensional NMR, Circular Dichroism, and Fluorescence Studies of PP-50, a Synthetic ATP-Binding Peptide from the β-Subunit of Mitochondrial ATP Synthase†

Woei-Jer Chuang, Chitrananda Abeygunawardana, Peter L. Pedersen, and Albert S. Mildvan*

Department of Biological Chemistry, The Johns Hopkins University School of Medicine, 725 North Wolfe Street, Baltimore, Maryland 21205

Received February 21, 1992; Revised Manuscript Received June 2, 1992

ABSTRACT: PP-50, a peptide based on residues 141–190 of the β-subunit of mitochondrial F_1-ATPase, contains the GX_4GKT consensus region for nucleoside triphosphate binding and has been shown to bind ATP [Garboczi, D. N., Shenbagamurthi, W. K., Hullihen, J., & Pedersen, P. L. (1988) *J. Biol. Chem. 263,* 812–816]. At pH 4.0, appropriate for NMR studies, PP-50 retains the ability to bind ATP tightly (K_D = 17.5 μM) with a 1:1 stoichiometry as shown by titrations measuring the partial quenching of ATP fluorescence by PP-50. CD spectra of PP-50 at pH 4.0 and at low ionic strength show 5.8% helix, 30.2% β-structure, and 64% coil. ATP binding increases the structure of PP-50, changing the CD to 7.5% helix, 44.5% β-structure, and 48% coil. Increasing the ionic strength to 50 mM KCl also increases the structure, changing the CD to 7.4% helix, 64.4% β-structure, and 28.2% coil. The 600-MHz proton NMR spectrum of PP-50, at pH 4.0 and low ionic strength, has been assigned by 2D methods (TOCSY, DQF-COSY, and NOESY with jump-return water suppression). Based on strong $d_{\alpha N}$ NOEs, $J_{\alpha N}$ values, and NH chemical shifts differing from random coil values, regions of extended structure are detected from residues 1–7 and 43–48. Based on d_{NN}, $d_{NN(i,i+2)}$, and $d_{\alpha N(i,i+2)}$ NOEs and $^3J_{\alpha N}$ values, possible type I′ and type I turns are found from residues 11–14 and 31–34, respectively. However, the NMR data also show $d_{\alpha N}$ NOEs indicating extended structure throughout the peptide, suggesting that PP-50 in solution may have two principal conformations which interconvert rapidly on the NMR time scale, one involving turns from residues 11–14 and 31–34 and another with an extended conformation. Remote NOEs are found from Val-42 to Gly-13 and to Thr-23, indicating transient tertiary structure. Residues 16–23, consisting of the GX_4GKT consensus sequence for nucleoside triphosphate binding show $d_{\alpha N}$ NOEs, unshifted α- and β-proton resonances, and some averaged $^3J_{\alpha N}$ values indicating both extended structure and a random coil, hence flexibility in this region.

Mitochondrial ATP synthase which synthesizes ATP coupled to an electrochemical gradient of protons generated by the electron–transfer chain consists of two large proteins, F_o and F_1 (Pedersen & Amzel, 1985; Penefsky & Cross, 1991). The transmembrane protein F_o, has three subunits, a, b, and c, and is believed to function as a proton pathway in ATP synthesis and hydrolysis. The catalytic portion of the ATP synthase, F_1, consists of five different subunits in the stoichiometric ratio $\alpha_3\beta_3\gamma\delta\epsilon$ (Pedersen & Amzel, 1985; Penefsky & Cross, 1991). The β-subunits are generally believed to make a major contribution to ATP binding at the catalytic sites (Penefsky & Cross, 1991).

Several laboratories have noted sequence homologies between the β-subunit of F_1, and some ATP- and GTP-binding proteins such as adenylate kinase, myosin, elongation factor Tu and *ras* proteins, and ATP or GTP have been found to bind at these homologous regions (Fry et al., 1985, 1986; Dreusicke, 1988; Pai et al., 1989; Jurnak, 1985; Saraste et al., 1990). The primary structure of the nucleotide binding site typically contains a glycine-rich loop with a GX_4GKT (or S) consensus sequence. Based on X-ray and NMR studies of ATP- and GTP-binding proteins (Dreusicke, 1988; Pai et al., 1989; Jurnak, 1985; Fry et al., 1986; Redfield & Papastavros, 1990), the conserved lysine plays an important role in the conformation of the glycine-rich loop and may interact directly with one or more phosphates of the bound nucleotide.

In order to understand the substrate binding domain of the mitochondrial ATP synthase, PP-50, a peptide based on residues 141–190 of the β-subunit of F_1, has been synthesized, and its interactions with ATP, TNP–ATP, and a variety of other ligands have been studied (Garboczi et al., 1988). In this paper two-dimensional NMR, CD,[1] and fluorescence spectroscopies have been used to study the secondary structure and the affinity of PP-50 for ATP and its analogs.

MATERIALS AND METHODS

Peptide Synthesis and NMR Sample Preparation. PP-50 was synthesized on an Applied Biosystems Model 430A peptide synthesizer by the solid-state method (Merrifield, 1968) and was purified by HPLC on a semipreparative C18 column, as described previously (Garboczi et al., 1988). Peptide samples for NMR experiments were dissolved in H_2O at a concentration of 2.0 mM, and the pH was adjusted to 4.0 with small amounts of 100 mM KOH. For studies in H_2O, 10% D_2O was added for field/frequency locking. For studies in D_2O, the pH-adjusted sample was lyophilized and redissolved in 99.96% D_2O twice. All samples were passed over Chelex 100 (Bio-Rad) to remove trace paramagnetic metal ion

† Supported by National Institutes of Health Grants DK28616 (to A.S.M.) and CA10951 (to P.L.P.).

* To whom correspondence should be addressed.

[1] Abbreviations: CD, circular dichroism; DQF-COSY, double quantum filtered correlated spectroscopy; TOCSY, total correlated spectroscopy; NOESY, nuclear Overhauser effect spectroscopy.

0006-2960/92/0431-7915$03.00/0

contaminants. If necessary, further adjustment of the pH with KOD or DCl was subsequently carried out.

NMR Spectroscopy. All proton NMR spectra were obtained at 600 MHz with a Bruker AM 600 NMR spectrometer. The data were processed on an Aspect 3000 computer and on a personal IRIS (Silicon Graphics Inc.) using the software FELIX (Hare Research Inc.). All 2D NMR spectra were recorded in the phase-sensitive absorption mode with quadrature detection in both F1 and F2 dimensions (Marion & Wüthrich, 1983). In 2D NMR experiments, the spectral widths were 8064 Hz in 90% H_2O/10% D_2O and 6024 Hz in 99.96% D_2O. Both DQF-COSY (Rance et al., 1983) and TOCSY spectra (Braunschweiler & Ernst, 1983) were acquired with presaturation of the water resonance during the relaxation delay (1–2 s). The MLEV 17 pulse sequence (Bax & Davis, 1985) was used to produce a spin-lock period of 69.5 ms for the TOCSY experiments. NOESY spectra (Jeener et al., 1979) were acquired with mixing times of 100, 200, and 300 ms and a relaxation delay of 1 s. The water resonance was suppressed by replacing the detection pulse with a $90°_x$–τ–$90°_x$, jump-return pulse sequence (Plateau & Gueron, 1982), permitting the detection of resonances near the water resonance.

A total of 4096 complex data points were acquired in F2 with acquisition times of either 0.254 or 0.340 s. Between 400 and 800 increments were acquired in F1 and 64–128 scans per increment were used depending on the experiment performed. The time domain data sets were zero-filled in F1 to 1024 points and were multiplied in both dimensions by a squared sine-bell function shifted by 45–60° prior to the Fourier transformation. Linear base line correction was generally applied in the F2 direction after Fourier transformation.

Fluorescence Titrations. The fluorescence of $(H^+)_2ATP$ at pH 4.0 was measured on a Perkin-Elmer 650–10S fluorescence spectrophotometer by exciting at 240 nm and observing from 300 to 450 nm. A solution of 12.55 μM ATP in 5 mM sodium acetate buffer, pH 4.0, at 27 °C was titrated with a 344 μM stock solution of PP-50 containing 12.55 μM ATP monitoring the decreasing fluorescence of $(H^+)_2ATP$. A 0.3-cm cuvette was used, and the initial and final volumes of the solution were 110 and 170 μL, respectively. At each concentration of PP-50, the weak fluorescence of $(H^+)_2ATP$ was determined by integrating the emission spectrum from 300 to 450 nm, and the dissociation constant and binding stoichiometry were obtained by computer fitting the data to a titration curve as previously described (Mullen et al., 1989).

The strong fluorescence of TNP–ATP at pH 7.5 was measured by exciting at 410 nm and observing at the emission maximum of 540 nm. A solution of 7.6 μM PP-50 in 10 mM Tris buffer, pH 7.5, at 27 °C was titrated with a 114 μM stock solution of TNP–ATP containing 7.6 μM PP-50 (to avoid dilution of the peptide), monitoring the fluorescence increase of TNP–ATP. In competition experiments, 5 mM ATP was added to the PP-50 solution prior to titration with a solution containing TNP–ATP and all other components of the system to avoid dilution.

CD Spectroscopy. CD spectra were measured at 27 °C on an AVIV 60DS spectropolarimeter that had been calibrated with camphosulfonic acid (Chen & Yang, 1977). Spectra were recorded between 185 and 260 nm using a 0.1-mm quartz cell. The samples contained PP-50 (172 μM), PP-50 with ATP (183 μM), and PP-50 with KCl (50 mM) at pH 4.0. A 1.0-nm spectral step size, a 1.0-nm band width, and a 12 nm/min scan rate was employed. In studying the effects of dilution on CD spectra, a 2-mm quartz cell was used. The final spectra obtained were the average of five scans, and were corrected by subtraction of five scans of the solvent alone. The ellipticity is reported as the mean residue ellipticity, θ (in units of deg cm^2/dmol). The secondary structure of PP-50 was estimated by using the CCAFAST and LINCOMB software (Perczel et al., 1991, 1992) generously provided by Dr. G. D. Fasman together with their basis set of 25 protein spectra. Attempts to fit the CD data were also made by using the basis sets of Yang et al. (1986) and Stone et al. (1985).

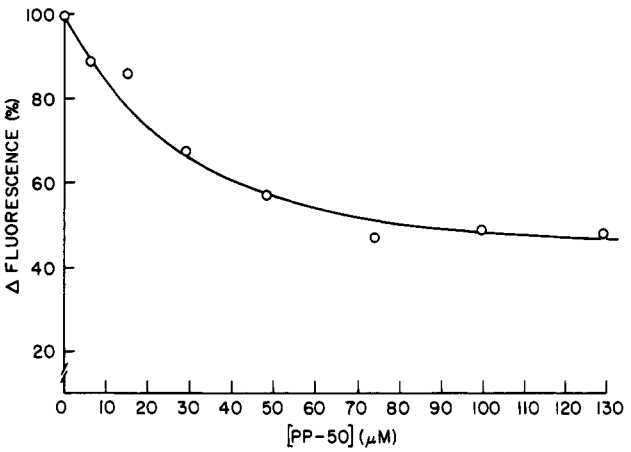

FIGURE 1: Fluorescence titration of H_2ATP^{2-} with PP-50. Components present were ATP (12.6 μM) and 5.0 mM sodium acetate buffer, pH 4.0, T = 27 °C. Conditions are otherwise as described in the Materials and Methods section. The data were fitted to a titration curve with a mean deviation of ±1.3% as previously described (Mullen et al., 1989), assuming a 1:1 stoichiometry, a K_D of 17.5 μM, and 60% quenching of H_2ATP^{2-} fluorescence in the complex.

RESULTS

Fluorescence Titrations of PP-50. PP-50 has previously been shown to interact with the fluorescent ATP analog TNP–ATP at pH 7.4, increasing the fluorescence of TNP–ATP, and the presence of ATP was shown to decrease the binding of TNP–ATP to PP-50 (Garboczi et al., 1988). We have confirmed these findings. Because of the tendency of PP-50 to aggregate in the presence of nucleotides at neutral pH, substoichiometric binding of TNP–ATP to PP-50 was observed (Garboczi et al., 1988). At pH 4.0, appropriate for NMR studies, PP-50 does not aggregate and H_2ATP^{2-} which exists at this pH (pK_a = 4.1) is itself fluorescent due to protonation at the N1 of adenine, permitting the direct titration of H_2ATP^{2-} with PP-50. Such a titration, monitoring the decreasing fluorescence of H_2ATP^{2-} by PP-50 (Figure 1) shows that at pH 4.0 PP-50 retains the ability to bind ATP tightly (K_D = 17.5 μM), with a 1:1 stoichiometry, quenching its fluorescence by 60%.

CD Spectroscopy of PP-50. CD spectroscopy was used to determine the secondary structure of PP-50 alone (172 μM), in the presence of KCl (50 mM), and in the presence of H_2ATP^{2-} (183 μM). The CD spectra were fit with a root mean square deviation (RMSD) of 2.9–5.4% using the convex constraint algorithm (CCA) together with a least-square-fit program (LINCOMB) of Perczel et al. (1991, 1992). This method eliminates the contributions from the dichroism of the aromatic amino acids. Analysis of the CD spectra of PP-50 alone (Figure 2A) shows 5.8% helix, 30.2% β-structure, and 64% coil. The secondary structure of the ATP-PP-50 complex (Figure 2B) consists of 7.5% helix, 44.5% β-structure, and 48% coil, indicating a change from coil to β-structure for PP-50 in the 1:1 complex with ATP. Interestingly, a dramatic change from coil to β-structure is also found for PP-50 in the

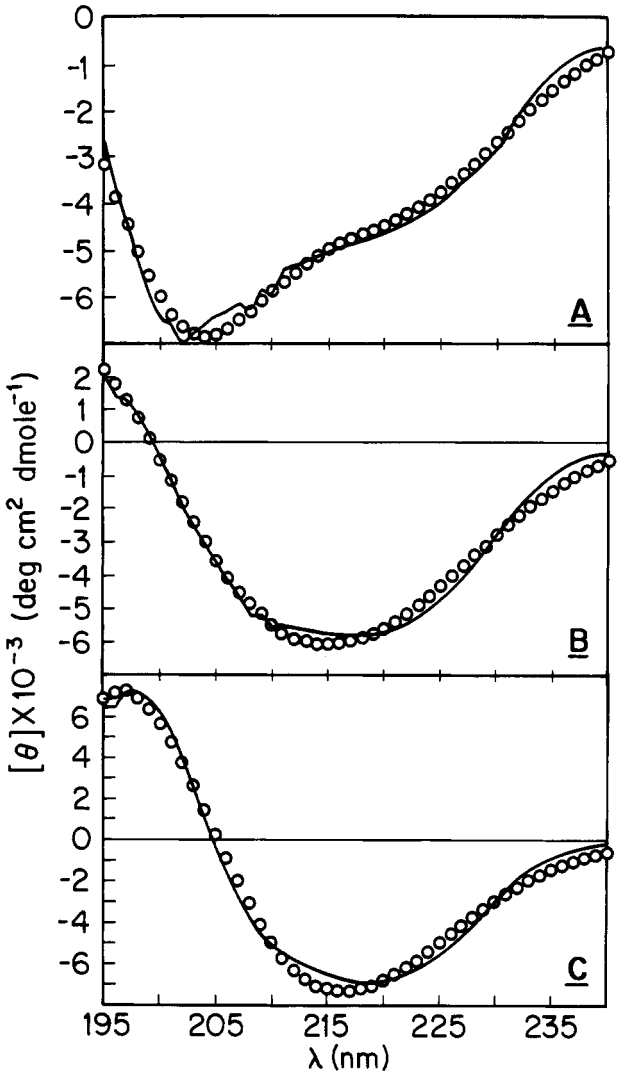

FIGURE 2: CD spectra of PP-50 in H_2O. (A) PP-50 alone (172 μM). (B) PP-50 with ATP (183 μM). (C) PP-50 with KCl (50 mM). Conditions were pH 4.0, $T = 27$ °C. Shown are the data (O) together with theoretical curves calculated by the LINCOMB program. The RMSD values are 3.2, 5.4, and 2.9%, respectively.

presence of 50 mM KCl (Figure 2C). Under these conditions, the secondary structure of PP-50 contains 7.4% α-helix, 64.4% β-structure, and 28.2% coil.

The CD spectra of Figure 2 were also analyzed by using the basis sets of Stone et al. (1985) and of Yang et al. (1986). However, the root mean square deviations were much larger (>12%) although these basis sets extended into the far-UV region. Recently, Yang showed that CD data truncated at 190 nm can also give reasonable estimates of secondary structure (Venyaminov et al., 1991). Ten- and 20-fold decreases in the concentration of PP-50 from 200 to 20 μM and 10 μM, together with compensatory increases in the light path from 0.1 to 1.0 and 2.0 mm, respectively, had little or no effect on the shape of the CD spectrum, the location of the minimum at 204 nm, or in the computed secondary structural contributions, within their experimental errors of 3–6%, arguing against significant aggregation over this range of concentrations.

NMR Spin System Assignment. The two-dimensional proton NMR spectra of PP-50 (2 mM) were acquired at pH 4.0 and 27 °C. The spin systems were assigned using a standard approach by analyzing the scalar connectivities in DQF-COSY and TOCSY spectra (Wüthrich, 1986). The

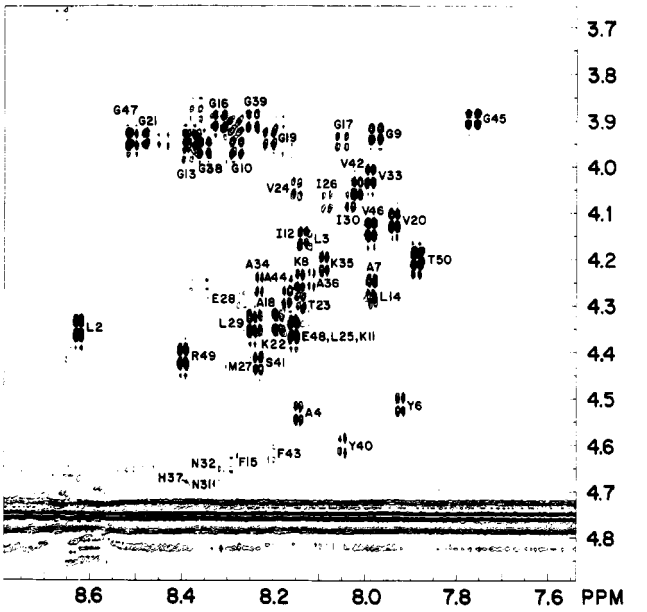

FIGURE 3: DQF-COSY spectrum of PP-50. The αH–NH fingerprint region from a double quantum filtered COSY spectrum of PP-50 is shown. The data sets were multiplied in both F1 and F2 dimensions by a 45° shifted squared sine-bell function prior to the Fourier transformation. The peaks are labeled with the residue symbols according to spectral assignments. Conditions are otherwise as described in the Materials and Methods section.

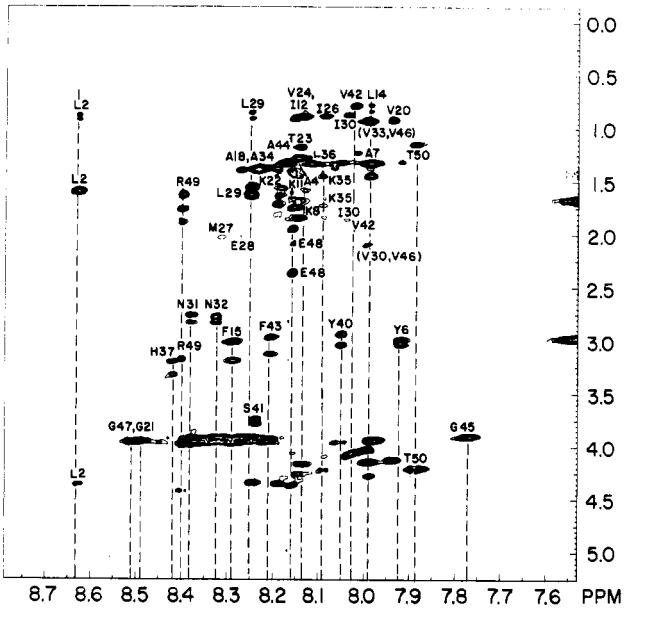

FIGURE 4: TOCSY spectrum of PP-50 in H_2O. The NH (F2) and aliphatic (F1) region of PP-50 in H_2O is shown. The data sets were multiplied in both F1 and F2 dimensions by a 45° shifted squared sine-bell function prior to Fourier transformation. Conditions are otherwise as described in the Materials and Methods section.

correlations in the NH–αH region of the DQF-COSY in H_2O (Figure 3), the NH–aliphatic region of the TOCSY in H_2O (Figure 4), and the αH–aliphatic region of the TOCSY in D_2O (Figure 5) were used to assign NH and αH protons.

The TOCSY spectrum in H_2O (Figure 4) has been used to assign many spin systems by total J-correlation from the backbone NH through to the terminal side-chain protons. PP-50 contains six alanines, five valines, five leucines, and three isoleucines leading to considerable overlap of resonances in DQF-COSY spectra. However, with the help of the TOCSY spectrum in H_2O (Figure 4) and in D_2O (Figure 5),

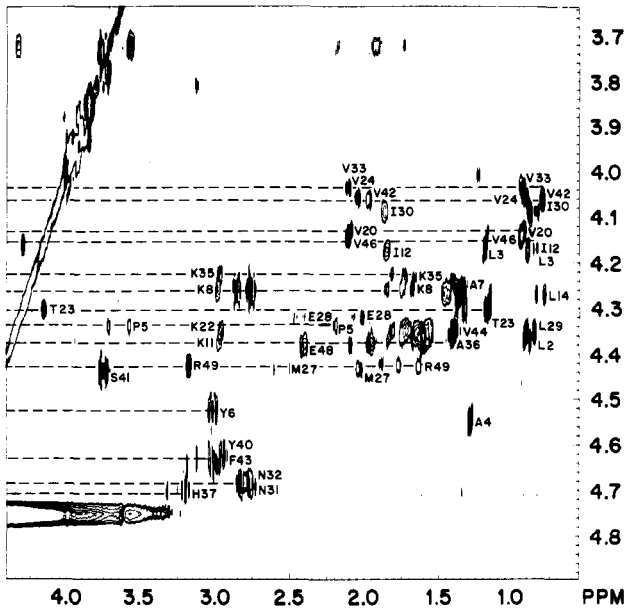

FIGURE 5: TOCSY spectrum of PP-50 in ^2H_2O. The aliphatic (F2) and αH (F1) region of PP-50 in ^2H_2O is shown. The data sets were multiplied in both F1 and F2 dimensions by a 45° shifted squared sine-bell function prior to Fourier transformation. Conditions are otherwise as described in the Materials and Methods section.

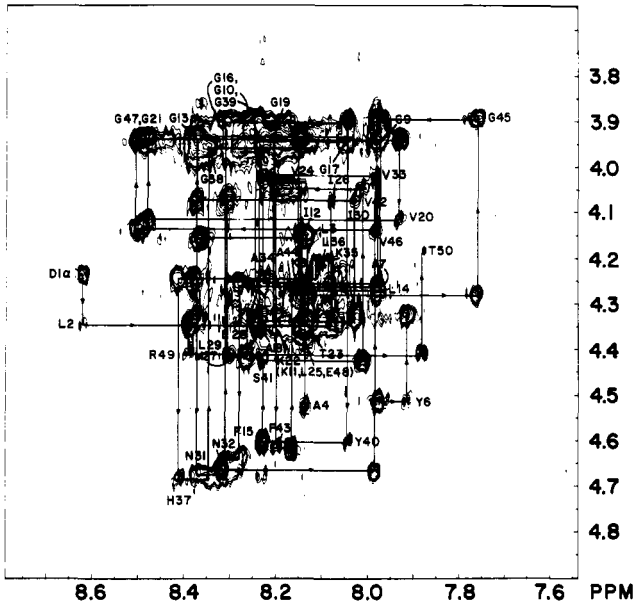

FIGURE 6: NOESY spectrum of PP-50. The αH-NH fingerprint region from a NOESY spectrum of PP-50 with 300 ms mixing time is shown. The data sets were multiplied in both F1 and F2 dimensions by a 60° shifted squared sine-bell function prior to Fourier transformation. Conditions are otherwise as described in the Materials and Methods section.

the ambiguities due to partial overlap in the upfield aliphatic region can be resolved.

NMR Sequential Assignment. NOESY spectra were acquired with mixing times of 100, 200, and 300 ms to assure the amplitude of the through space αH to NH connectivities and to attenuate possible spin diffusion. Sequential assignment was made by identifying sequential αH_i–N_{i+1} connectivities in the NOESY spectra (Figure 6).

The sequential assignments (Table I) were started from the carboxy-terminal T50 αH–NH cross peak. Sequential NOEs were unambiguously traced back to the Y40NH and the G39αH cross peak. It was difficult to assign the αH resonance of G39 because the αH of the 11 glycines disperse only between 3.89 and 3.96 ppm. However, the ambiguity was resolved by the strong cross peak between G39NH and G38αH. The pathway of $d_{\alpha N}$ connectivities from G38 through I26 was also readily identified. On assigning L25, the αH_i–NH_i cross peak of L25 was found to overlap with that of E48. A weak $d_{\alpha N}$ NOE was identified between L25 and V24, and was verified by a strong γH_i–NH_{i+1} NOE. The sequence connectivity was traced accurately from V24 to I12. The αH_i–NH_i cross peak of K11 also overlaps with those of E48 and L26, but sequential αH_i–NH_{i+1} NOEs involving these residues could clearly be identified. All remaining connectivities were readily identified except for the break between P5 and A4. The αH of P5 was identified from the TOCSY in D_2O (Figure 5). A small number of NH–NH NOEs were also observed (Figure 7) which confirmed some of the sequential assignments and provided additional structural information.

NMR Structural Analysis. Secondary structural information and backbone interresidual NOEs are summarized in Figure 8. The PP-50 sequence is represented by the one-letter code. The chemical shift differences of NH, αH, and βH resonances relative to those of random coil values (Wüthrich, 1986) are represented by the thickness of the blocks. Most chemical shifts of PP-50 are significantly changed in comparison with those of a random coil. The correlation between NOEs and the secondary structure of proteins has been well established (Wüthrich, 1986). Most short linear peptides exist in a state of conformational equilibrium (Dyson & Wright, 1991). Highly fluctuating peptides generally are characterized by random coil chemical shifts (Kessler & Bermel, 1986), by similar magnitude $d_{\alpha N}$ NOEs and absent d_{NN} NOEs, and by random coil $^3J_{\alpha N}$ coupling constants. PP-50 shows some preferred possibly transient structures from the observation of d_{NN}, $d_{NN(i,i+2)}$, $d_{\alpha N(i,i+2)}$, and two long-range NH–NH NOEs, from residues 13 → 42 and 23 → 42 (Figure 7), largely nonaveraged coupling constants, and nonrandom coil chemical shifts (Figure 8). The proximity of Val-42 to Gly-13 is confirmed by NH–αH NOEs of medium intensity observed both in 200- and 300-ms NOESY spectra in H_2O and by weak αH–αH NOEs in a 300-ms NOESY spectrum in D_2O. The proximity of Val-42 to Thr-23 is confirmed by weak γH–αH NOEs in a 300-ms NOESY spectrum in D_2O.

Based on strong $d_{\alpha N}$ NOEs, $J_{\alpha N}$ values, and NH chemical shifts differing from random coil values, regions of extended structure are detected from residues 1–7 and 43–48. Based on d_{NN}, $d_{NN(i,i+2)}$, and $d_{\alpha N(i,i+2)}$ NOEs, a possible type I′ turn is found from residues 11–14 and a possible type I turn is found from residues 31–34. Residues 16–23, consisting of the GX_4GKT consensus sequence, show strong $d_{\alpha N(i,i+1)}$ NOEs indicating extended structure yet unshifted α and β proton resonances and, in residues 20–22, averaged $^3J_{\alpha N}$ values suggesting a random coil, hence flexibility in this region. PP-50 also shows some d_{NN} NOEs (L36 → G38, A7 → G10, I26 → E28, and G13 → V42) (Figure 7) and $d_{\beta N(i,i+1)}$ NOEs, which further indicate that PP-50 has some preferred transient conformation in aqueous solution.

The NOESY spectra thus show not only NOEs characteristic for turns between residues 11–14 and 31–34 but also medium to strong $d_{\alpha N(i,i+1)}$ NOEs throughout, except at P5 and at the N-terminal residue, indicating that PP-50 in solution may have two principal sets of conformations: a set of extended conformations and a set of conformations consisting of type I′ and type I turns from residues 11–14 and 31–34, respectively. These two sets of conformations interconvert rapidly on the

Table I: Proton Chemical Shifts (ppm) and $^3J_{\alpha N}$ (Hz) of PP-50

no.	amino acid	NH	αH	βH	γH	δH	εH	others	$^3J_{\alpha N}$
1	Asp		4.25	2.87, 2.77					
2	Leu	8.63	4.35	1.60	1.60	0.90, 0.86			6.0
3	Leu	8.13	4.15	1.59	1.59	0.85, 0.90			
4	Ala	8.15	4.53	1.28					5.9
5	Pro		4.33	1.74, 2.18	1.94	3.71, 3.96			
6	Tyr	7.93	4.51	3.00, 3.04				2,6H 7.11, 3,5H 6.79	7.4
7	Ala	7.99	4.26	1.34					7.0
8	Lys	8.14	4.24	1.85, 1.75	1.44, 1.46	1.68	2.98	ϵNH_3^+ 7.52	5.8
9	Gly	7.98	3.93						11.8
10	Gly	8.28	3.91, 3.96						11.8
11	Lys	8.17	4.35	1.84, 1.75	1.41, 1.40	1.66	2.98	ϵNH_3^+ 7.52	5.9
12	Ile	8.14	4.15	1.84	0.92				8.8
13	Gly	8.38	3.94						5.9
14	Leu	7.98	4.26	1.43	1.43	0.78, 0.84			4.4
15	Phe	8.28	4.64	3.19, 3.01				2,6H 7.25, 3,5H 7.40, 4H 7.10	5.9
16	Gly	8.32	3.90						11.8
17	Gly	8.06	3.94						11.7
18	Ala	8.24	4.32	1.38					
19	Gly	8.21	3.93						11.8
20	Val	7.94	4.12	2.09	0.92				5.9
21	Gly	8.49	3.94						5.8
22	Lys	8.19	4.33	1.82	1.40, 1.38	1.73, 1.66	2.96	ϵNH_3^+ 7.52	7.4
23	Thr	8.14	4.28	4.14	1.18				
24	Val	8.15	4.04	2.04	0.91				8.8
25	Leu	8.17	4.35	1.59	1.59	0.88, 0.90			5.9
26	Ile	8.09	4.07	1.84	0.89, 0.89				8.8
27	Met	8.32	4.42	2.02, 2.05	2.61, 2.61		2.17		6.9
28	Glu	8.28	4.31	2.02	2.40, 2.45				
29	Leu	8.25	4.15	1.55	1.63	0.85, 0.90			5.9
30	Ile	8.04	4.07	1.85	0.88, 0.88				8.8
31	Asn	8.39	4.66	2.75, 2.82				γNH_2 7.58, 6.90	5.9
32	Asn	8.32	4.66	2.76, 2.83				γNH_2 7.58, 6.90	6.0
33	Val	7.99	4.02	2.10	0.94				7.9
34	Ala	8.23	4.26	1.37					6.0
35	Lys	8.09	4.21	1.82	1.40	1.73, 1.66	2.97	ϵNH_3^+ 7.52	7.4
36	Ala	8.12	4.24	1.32					5.9
37	His	8.42	4.65	3.20, 3.32				2H 8.63, 4H 7.32	5.9
38	Gly	8.36	3.96						8.8
39	Gly	8.25	3.90						8.2
40	Tyr	8.05	4.60	3.04				2,6H 7.09, 3,5H 6.80	5.9
41	Ser	8.24	4.42	3.73, 3.78					7.4
42	Val	8.03	4.04	1.96	0.78				8.8
43	Phe	8.21	4.62	3.01, 3.19				2,6H 7.24, 3,5H 7.30, 4H 7.25	8.0
44	Ala	8.18	4.28	1.32					6.9
45	Gly	7.77	3.89						11.8
46	Val	7.99	4.13	2.10	0.93				8.9
47	Gly	8.51	3.94						11.8
48	Glu	8.17	4.35	2.09, 1.97	2.40, 2.39				5.9
49	Arg	8.40	4.41	1.88, 1.77	1.62, 1.62	3.18, 3.19		NH 7.11, 6.82	6.0
50	Thr	7.89	4.19	4.19	1.16				8.8

NMR (NOE) time scale. A summary of the transient structure is given by the diagram of Figure 9.

DISCUSSION

A nucleotide-binding domain of the mitochondrial synthase, PP-50, a peptide based on residues 141–190 of the β-subunit of F_1 has been shown to interact with ATP and TNP–ATP by fluorescence titrations. At pH 4.0, appropriate for NMR studies, PP-50 retains the ability to bind ATP tightly (K_D = 17.5 μM) and stoichiometrically. Interestingly, the intact F_1-ATPase from liver, on which this peptide is based, binds three molecules of AMPPNP reversibly with dissociation constants ranging from 1.2 to 26 μM at pH 7.5 (Williams et al., 1987).[2] On the basis of CD spectral analysis, PP-50 contains 64% coil and the binding of the substrate ATP increases the β-structure at the expense of random coil, indicating that the structure and rigidity of PP-50 has been increased by binding with ATP. At the 12-fold greater concentrations of PP-50 needed for the NMR studies, the presence of ATP induced precipitation of the peptide.

Two-dimensional proton NMR spectroscopy has been used to assign all of the resonances in PP-50. Most short peptides are present in solution as an ensemble of rapidly interconverting conformers (Dyson & Wright, 1991). The NOEs reflect a population-weighted average over all conformers and only distinguish the conformers that interconvert on a millisecond-to-second time scale. On the basis of the present NOEs, PP-50 consists of a set of extended conformers and a set of conformers with type I′ and type I turns. The study by Osterhaut et al. (1989) is another example of such a conformational equilibrium for a 24-residue peptide.

Peptide fragments of proteins in aqueous solution, in many cases, exhibit significant conformational preferences for recognizable structure (Wright et al., 1988). Such studies provide structural insights about protein folding. In PP-50 the protein fragment has a stretch of amino acids with the

[2] Analysis of the Scatchard plot of Williams et al. (1987) for the binding of AMPPNP to F_1-ATPase, taking into account both the tight and the weak binding sites, yields a K_D = 1.2 μM for the one tight binding site and a K_D = 26 μM for the two weak binding sites.

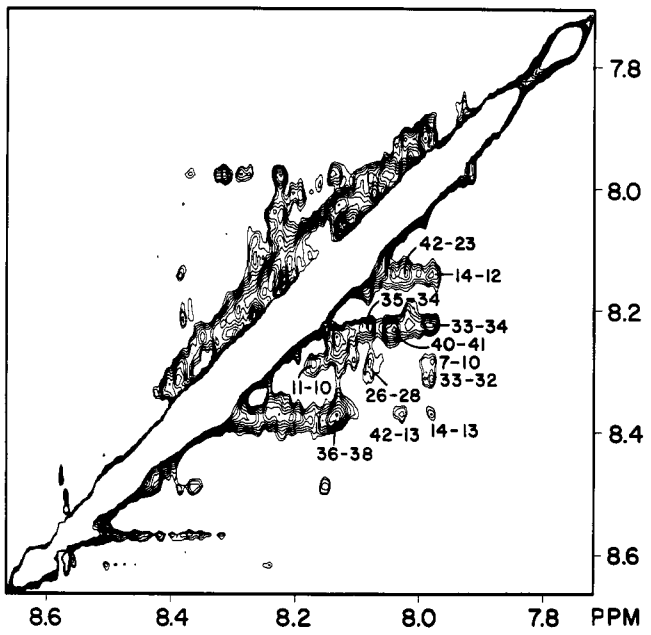

FIGURE 7: NOESY spectrum of PP-50. The NH–NH region of PP-50 in H_2O is shown. The data sets were multiplied in both F1 and F2 dimensions by a 60° shifted squared sine-bell function prior to Fourier transformation. The labeling of resonances is represented by column to row sequence.

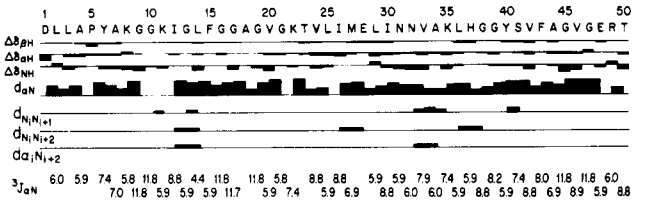

FIGURE 8: Summary of NMR data for PP-50. The chemical shift difference of NH, αH, and βH resonances relative to those of random coil values and intensity of NOEs are represented by the thickness of the blocks.

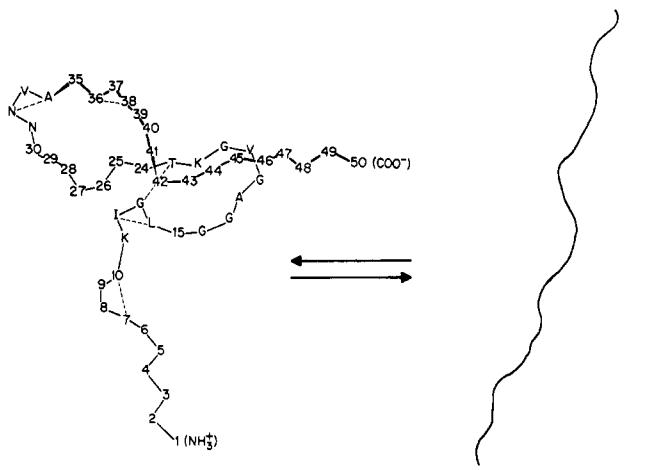

FIGURE 9: Diagram of the transient secondary structure of PP-50 based on short, intermediate, and long-range NOEs. Intermediate and long-range NOEs are indicated by dashed lines.

consensus GX_4GKT/S which shows homology with other nucleoside triphosphate binding loops. This protein motif has been called a flexible loop because of its high content of glycine residues. On the basis of our NMR studies, the loop is flexible (Figures 8 and 9), and from our CD studies the structure of the peptide, possibly including the loop, is increased by binding ATP. X-ray and NMR studies of other proteins implicate this loop as interacting with one or more phosphates of ATP (Fry et al., 1985, 1986; Dreusicke, 1988; Pai et al., 1989; Jurnak, 1985; Redfield & Papastavros, 1990).

Considerable evidence has accumulated in recent years which shows that peptide fragments of proteins in aqueous solution can transiently adopt folded structures (Wright et al, 1988). Incomplete folding of such peptides in aqueous solution results from hydrogen-bonding competition between backbone NH and C=O groups of polypeptide chains with water, difficulty the in formation of intramolecular hydrophobic clusters, and inappropriate electrostatic interactions between charged residues which are not part of the properly folded structure. Peptide fragments of proteins in aqueous solution thus do not have completely folded structures because of the differing folding environment. If the peptide fragment comes from the surface of the protein and is exposed to the aqueous surrounding, it may have a folded structure like that of the protein. On the basis of crystallographic studies of other proteins (Dreusicke, 1988; Pai et al., 1989; Jurnak, 1985), the glycine-rich loop is exposed to the aqueous surroundings, indicating that the structural studies of PP-50 in aqueous solution can provide insights about nucleotide-binding sites in proteins.

ACKNOWLEDGMENT

We are grateful to P. Shenbagamurthi for synthesizing PP-50, to D. R. Shortle for the use of the CD spectrometer, to G. P. Mullen and Wu-Schyong Liu for helpful discussions, and to P. Ford for secretarial assistance.

REFERENCES

Bax, A., & Davis, D. G. (1985) *J. Magn. Reson. 65*, 355–360.
Braunschweiler, L., & Ernst, R. (1983) *J. Magn. Reson. 53*, 521–528.
Chen, G. C., & Yang, J. T. (1977) *Anal. Lett. 10 (14)*, 1195–1207.
Dreusicke, D., Kauplus, P. A., & Schultz, G. E. (1988) *J. Mol. Biol. 199*, 359–371.
Dyson, H. J., & Wright, P. E. (1991) *Annu. Rev. Biophys. Biophys. Chem. 20*, 519–538.
Fry, D. C., Kuby, S. A., & Mildvan, A. S. (1985) *Biochemistry 24*, 4680–4694.
Fry, D. C., Kuby, S. A., & Mildvan, A. S. (1986) *Proc. Natl. Acad. Sci. U.S.A. 83*, 907–911.
Garboczi, D. N., Shenbagamurthi, W. K., Hullihen, J., & Pedersen, P. L. (1988) *J. Biol. Chem. 263*, 812–816.
Jeener, J., Meier, B. H., Bachmann, P., & Ernst, R. R. (1979) *J. Chem. Physics 71*, 4546–4553.
Jurnak, F. (1985) *Science 230*, 32–36.
Kessler, H., & Bermel, W. (1986) in *Methods in Stereochemical Analysis 6: Applications of NMR Spectroscopy to Problems in Stereochemistry and Conformational Analysis* (Takenchi, Y., & Marchand, A. P., Eds.) VCH, Deerfield Beach, FL.
Marion, D., & Wüthrich, K. (1983) *Biochem. Biophys. Res. Commun. 113*, 967–974.
Merrifield, R. B. (1968) *J. Am. Chem. Soc. 85*, 2149–2154.
Mullen, G. P., Shenbagamurthi, P., & Mildvan, A. S. (1989) *J. Biol. Chem. 264*, 19637–19647.
Osterhaut, J. J., Baldwin, R. L., York, E. J., Stewart, J. M., Dyson, H. J., & Wright, P. E. (1989) *Biochemistry 28*, 7059–7064.
Pai, E. F., Kabsch, W., Krengel, U., Holmes, K. C., John, J., & Wittinghofer, A. (1989) *Nature 341*, 209–214.
Pedersen, P. L., & Amzel, L. M. (1985) in *Bioenergetics* (Quagliariello, E., Ed.) Vol. VI, pp 169–189, Elsevier Science Publishers, New York.
Penefsky, H. S., & Cross, R. L. (1991) in *Advances in Enzymology and Related Areas of Molecular Biology* (Meister, A., Ed.) Vol. 64, pp 173–214, John Wiley & Sons, New York.

Perczel, A., Hollosi, M., Tusnady, G., & Fasman, G. (1991) *Protein Eng. 4*, 669–679.

Perczel, A., Park, K., & Fasman, G. D. (1992) *Anal. Biochem. 203*, 83–93.

Plateau, P., & Gueron, M. (1982) *J. Am. Chem. Soc. 104*, 7310–7311.

Rance, M., Sorensen, O. W., Bodenhausen, G., Wagner, G., Ernst, R. R., & Wüthrich, K. (1983) *Biochem. Biophys. Res. Commun. 117*, 479–485.

Redfield, A. G., & Papastavros, M. Z. (1990) *Biochemistry 29*, 3509–3514.

Saraste, M., Sibbald, P. R., & Wittinghofer, A. (1990) *Trends Biochem. Sci. 15*, 430–434.

Stone, A. L., Park, J. Y., & Martenson, R. E. (1985) *Biochemistry 24*, 6666–6673.

Venyaminov, S. Y., Baikalv, I. A., Wu, C.-S. C., & Yang, J. T. (1991) *Anal. Biochem. 198*, 250–255.

Williams, N., Hullihen, J., & Pedersen, P. L. (1987) *Biochemistry 26*, 162–169.

Wright, P. E., Dyson, H. J., & Lerner, R. A. (1988) *Biochemistry 27*, 7167–7175.

Wüthrich, K. (1986) *NMR of Proteins and Nucleic Acids*, John Wiley & Sons, New York.

Yang, Y. T., Wu, C.-S. C., & Martinez, H. M. (1986) *Methods Enzymol. 130*, 208–269.